Optical Rogue Waves in Whispering-Gallery-Mode Resonators

Aurélien Coillet[1], John Dudley[1],* Goëry Genty[2], Laurent Larger[1], and Yanne K. Chembo[1]
[1] *FEMTO-ST Institute [CNRS UMR6174], Optics Department, 16 Route de Gray, 25030 Besançon cedex, France.*
[2] *Tampere University of Technology, Institute of Physics, Optics Laboratory, FIN-33101 Tampere, Finland*
(Dated: January 9, 2014)

We report a theoretical study showing that rogue waves can emerge in whispering gallery mode resonators as the result of the chaotic interplay between Kerr nonlinearity and anomalous group-velocity dispersion. The nonlinear dynamics of the propagation of light in a whispering gallery-mode resonator is investigated using the Lugiato-Lefever equation, and we evidence a range of parameters where rare and extreme events associated with a non-gaussian statistics of the field maxima are observed.

PACS numbers: 42.62.Eh, 42.65.Hw, 42.65.Sf, 42.65.Tg.

Rogue (or "freak") waves are rare events of extreme amplitudes, that were first investigated in hydrodynamics where their fascinating nature and disastrous consequences have drawn noticeable attention. Further investigations have shown that rogue waves may arise in various nonlinear physical systems, including Bose-Einstein condensates, super-fluid helium and plasma waves (see for example ref. [1], and references therein). In optics, the first experimental observation of rogue waves was reported in 2007 [2], and since then, optical rogue waves have been the subject of extensive research activity in the context of super-continuum generation or laser systems (see [3–11] and references therein). The theoretical modelling of optical rogue waves in optical fibers is based on the generalized nonlinear Schrödinger equation (GNLSE), which includes various physical phenomena such as dispersion (second order and higher), dissipation, as well as Kerr and Raman nonlinearities. Here we provide theoretical evidence of rogue waves in whispering-gallery mode (WGM) resonators, resulting from the collision of soliton breathers in the process of hyperchaotic Kerr comb generation.

The system under study is schematically displayed in Fig. 1. A continuous-wave laser at 1550 nm is used to pump a whispering-gallery mode resonator which traps the photons by total internal reflection. In these resonators, the photon lifetime related to the resonance linewidth through $\tau_{\rm ph} = 1/\Delta\omega$, and it can be significantly high (typically, of the order of 1 μs for a loaded quality factor of $Q \sim 10^9$). In the fundamental familly of eigenmodes (doughnut-like modes), the confined laser radiation circulates in a torus inside the resonator. The eigenfrequencies of the WGM resonator can be Taylor-expanded as $\omega_\ell = \omega_{\ell_0} + \zeta_1(\ell-\ell_0) + \frac{1}{2}\zeta_2(\ell-\ell_0)^2$, where ℓ is the eigennumber which unambiguously labels all the modes of the fundamental family, ω_{ℓ_0} is the eigenfrequency of the pumped mode $\ell = \ell_0$, $\zeta_1 = d\omega/d\ell|_{\ell=\ell_0}$ is the free-spectral range of the resonator, and $\zeta_2 = d^2\omega/d\ell^2\big|_{\ell=\ell_0}$ is the second-order dispersion coefficient.

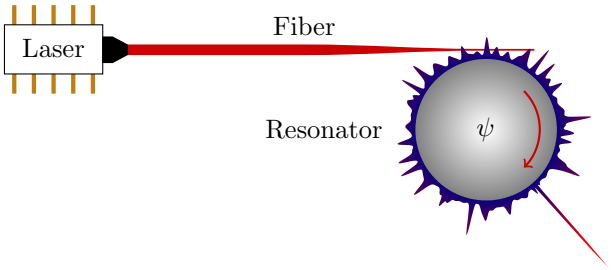

FIG. 1: (Color online) Schematic representation of the system under study. A continuous-wave laser radiation is coupled to a WGM cavity through the evanescent field of a tapered fiber. The WGM resonator can be a fused glass microsphere, a polished crystal disk, or an integrated resonator. Laser light is trapped by total internal reflection and travels along the azimuthally direction. The figure displays a snapshot of the numerical simulations that shows a rogue wave, which is in this case a sharp peak characterized by extreme amplitude and very rare occurrence.

It has been shown recently in refs. [12–14] that the spatiotemporal dynamics of the intra-cavity laser field can be modeled using the Lugiato-Lefever equation (LLE) [15], which is a NLSE with damping, driving and detuning:

$$\frac{\partial\psi}{\partial\tau} = -(1+i\alpha)\psi + i|\psi|^2\psi - i\frac{\beta}{2}\frac{\partial^2\psi}{\partial\theta^2} + F\,, \qquad (1)$$

where ψ is the normalized slowly-varying envelope of the intra-cavity field, $\tau = t/2\tau_{\rm ph}$ is the dimensionless time, and $\theta \in [-\pi,\pi]$ is the azimuthal angle along the circumference of the disk. The normalized parameter $\alpha = -2(\Omega_0 - \omega_{\ell_0})/\Delta\omega$ is scaling the physical detuning between the driving and the pumped eigenmode (Ω_0 and ω_{ℓ_0}, resp.), while the normalized parameter $\beta = -2\zeta_2/\Delta\omega$ is scaling the group-velocity dispersion (GVD) at the eigenmode frequency. We operate here in the regime of anomalous GVD which corresponds in the

*Corresponding author. E-mail: john.dudley@univ-fcomte.fr

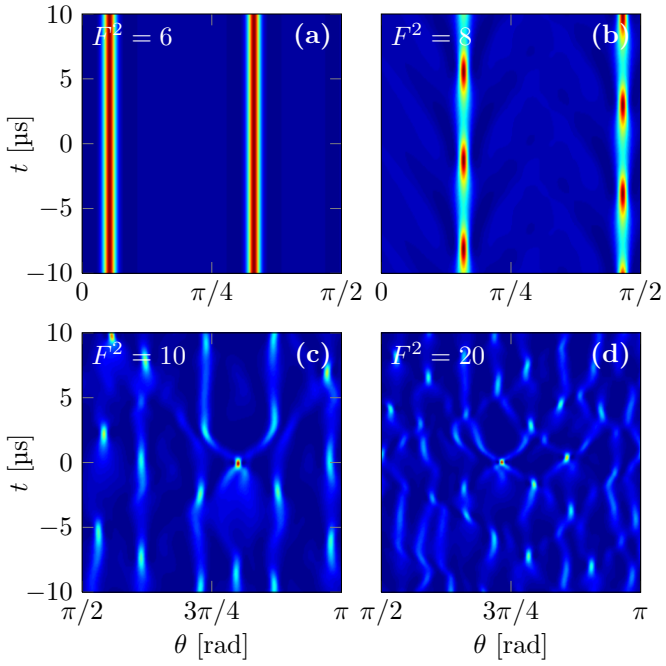

FIG. 2: (Color online) Spatio-temporal representation of the evolution of the optical field in the WGM resonator. For $F^2 = 6$, stable solitons emerge from the noisy initial condition, and remain stable. For $F^2 = 8$, soliton breathers are obtained. As the pump is increased ($F^2 = 10$ and 20), their number increases and they start to interact, thereby leading to unexpected, rare and extremely high amplitude waves. Note that only a fraction of the total cavity circumference is represented for better visibility. The burst of the highest wave of the simulation is chosen as the arbitrary time origin.

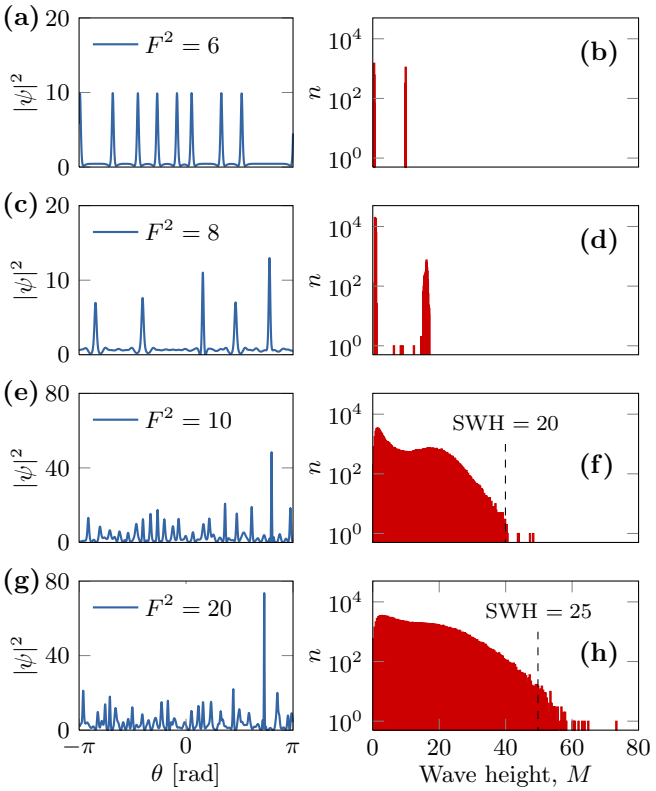

FIG. 3: (Color online) Left column: Spatial distribution of the optical intensity in the cavity when the highest wave occurs for different pump powers: $F^2 = \{6, 8, 10, 20\}$. It should be noted that this spatial representation in the moving frame inside the cavity will correspond to a temporal signal if the signal is coupled out of the resonator using an output coupler. Right column: The number of events recorded for each wave height bin is represented with a logarithmic scale for the vertical axis. The local maxima are extracted from the maps of Fig. 2 for each pump power. In the cases $F^2 = 10$ and $F^2 = 20$, the significant wave height (SWH) is calculated, and the black dashed lines correspond to twice this value.

model to $\beta < 0$. Finally, the square of the dimensionless pump term F in the LLE is proportional to the laser power P following:

$$F^2 = \frac{8g_0}{\hbar\Omega_0}\frac{\Delta\omega_{\text{ext}}}{\Delta\omega^3}P\,, \tag{2}$$

where $g_0 = n_2 c\hbar\Omega_0^2/n_0^2 V_0$ stands for the nonlinear gain, n_2 is the nonlinear refractive index of the material, V_0 is the effective volume of the pumped mode, and $\Delta\omega_{\text{ext}}$ is the contribution of the external coupling to the resonator linewidth. It is interesting to note that the intra-cavity field has been normalized in a way that $[\Delta\omega/2g_0]\,|\psi|^2$ is the total number of photons inside the resonator. The LLE modeling in the photonic WGM context has already been compared successfully with Kerr comb generation experiments [16], and is therefore a relevant theoretical tool to investigate the complex phenomenology of the laser field dynamics in the WGM resonator.

In optical fibers, extreme events generally arise in the regime of anomalous dispersion, where multiple bright solitons regime can be observed. In WGM resonators, bright solitons can also be generated for $\beta < 0$ and for detunings α greater than a critical value which is approximately equal to 2 [16, 17]. Here, we report the formation of rogue waves in WGM resonators pumped with a continuous-wave laser. It is found that pumping the system 10 times above the threshold for Kerr comb generation is sufficient to trigger complex chaotic-like (or turbulent) motion for which occurrence of rogue waves has been observed. Experimentally, this threshold power can be as low as a few milliwatts, and therefore, the pump power needed to obtain chaotic behavior can easily be reached [18, 19].

The LLE simulations are performed using the split-step Fourier method starting from random noise in the cavity. The WGM resonator's characteristics used for the simulations are $\beta = -0.0125$ and $Q = 3 \times 10^9$, corresponding to a loaded linewidth of $\Delta\omega/2\pi = 65$ kHz at the standard telecom wavelength $\lambda = 1550$ nm. The evolution of the field is simulated over 10 ms, a value

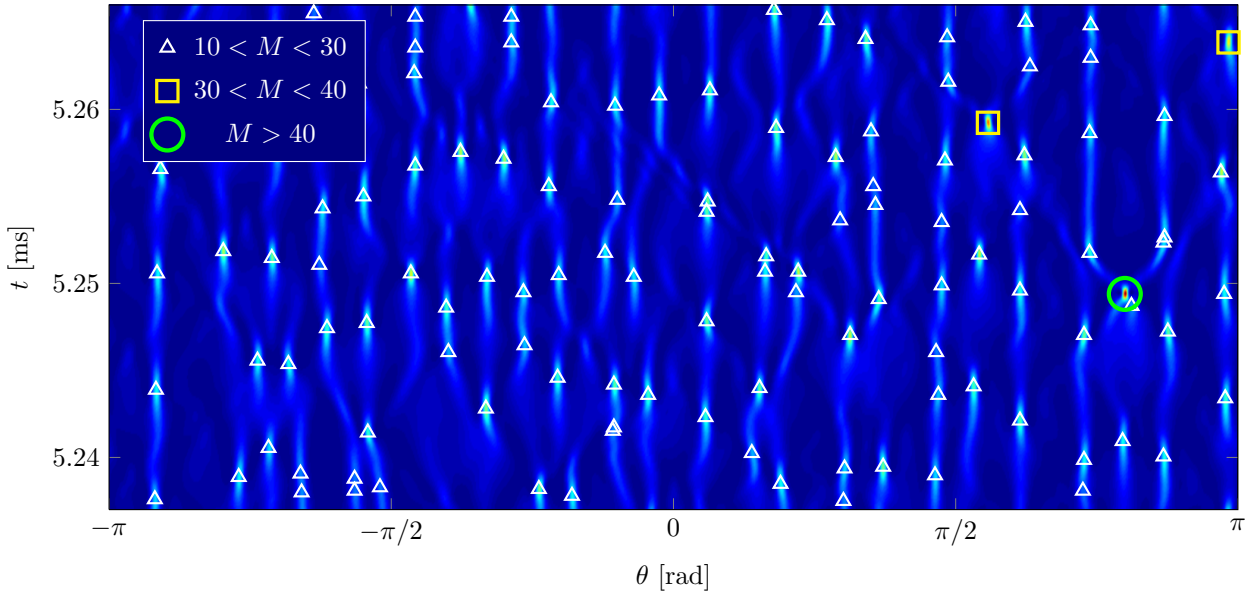

FIG. 4: (Color online) Evolution of the spatial distribution of the optical intensity inside the cavity with time. The frequency detuning is $\alpha = 4$ and excitation is set to $F^2 = 10$. Triangles are indicating the spatiotemporal location of local maxima whose amplitude M is between 10 and 30, corresponding to soliton breathers' maxima. The yellow square marks are higher intensity wave laying in the exponential tail of the statistical distribution; they correspond to moderate interaction between solitons. The green circle marks the highest wave of this simulation snapshot, and its extreme amplitude makes it lies outside of the exponential tail of the statistical distribution. This unexpected and very strong peak is a sample of what has been identified as a rogue wave in a laser-pumped WGM.

much higher than the photon lifetime of the cavity $\tau_{\rm ph} = 7.75$ μs. The transient dynamics is not concerned in our investigation, since we are expecting to obtain rogue waves as rare events of an asymptotic solution of the dynamics. Therefore the first millisecond of the simulation is removed from the time series used for the statistical analysis of the wave height. The resulting data consists in the evolution of the field intensity with time for each angle in the azimuthal direction of the resonator; a color-coded version of a portion of this map is represented in Fig. 2. Each map corresponds to a different value of the pump power $F^2 = \{6, 8, 10, 20\}$, while the detuning is kept constant at $\alpha = 4$.

The next step of our analysis consists in finding the local maxima of the optical field inside the cavity. It is worth noting that the minimum pump power leading to Kerr comb generation can theoretically be calculated as $F^2_{\rm th} = 1$ for $\alpha = 1$ (modulational instability leading to Turing patterns [16]). Hence, the values of the pump parameters that are considered in the present article ($F^2 < 20$) correspond to realistic pump power values ($P < 1$ W) that can be easily reached. In the first column of Fig. 3, we plot the spatial distribution of the optical field along the azimuthal direction of the cavity when the highest waves are recorded. On the second column, the statistical distribution of the wave heights is presented with a logarithmic scale in the ordinate. When the pump is fixed to $F^2 = 6$, solitons emerge from the initial noise in the cavity. This regime has already been investigated both theoretically [16, 17] and experimentally [20]. In terms of wave height distribution, this regime is characterized by two distinct levels, the soliton maximum and the small pedestal around them. When the pump power is increased, these solitons become unstable and soliton breathers are formed ($F^2 = 8$) [21]. In this case, the probability distribution of the wave heights is also given by two peaks histogram corresponding to the maxima of the breathers and the ripples between them. When the driving is further increased ($F^2 = 10$), the soliton breathers start to interact one with each other seldom resulting in the occurrence of intense and sharp pulses. At this point, the statistical distribution of the peaks height becomes continuous, but still displays the previously mentioned features corresponding to the breathers' maxima and ripples. The distribution tail for intense events exhibits a specific feature: an exponential decay characterizes the tail up to some threshold height (dashed line), above which one clearly sees very rare events that qualify for the appellation of "rogue waves".

The same behavior is also observed for higher pump power, at $F^2 = 20$ for instance, where several extreme events have been observed. The optical intensity in the cavity when the highest wave occurs is plotted in Fig. 3. This wave clearly stands above the others, and results from the interaction between previous soliton breathers. The statistical distribution of this simulation shows that

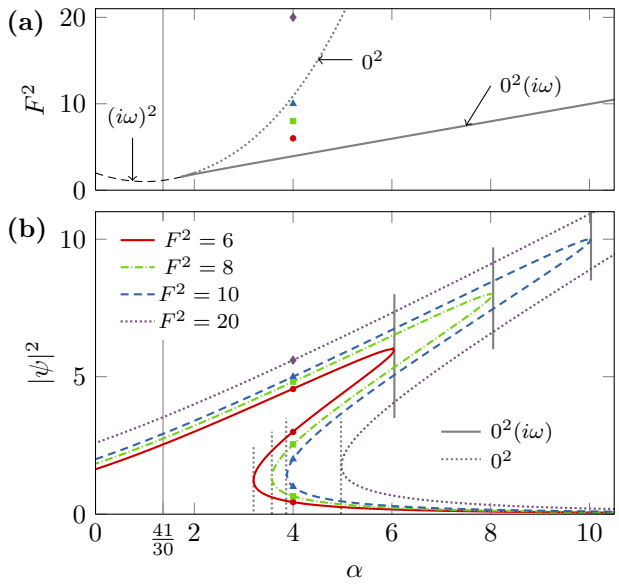

FIG. 5: (Color online) (a) Stability diagram of the LLE in the parameter space $\alpha - F^2$. The curves correspond to different bifurcations occurring for the angle-independent fixed points ψ_0. The markers represent the different simulations presented previously, and rogue waves are observed in the vicinity and above the 0^2 bifurcation line. (b) Nonlinear resonance profiles for different pump powers. Entry and exit from the hysteresis area occur through 0^2 and $0^2(i\omega)$ bifurcations respectively [22, 23]. Rogue waves observed in our case are observed for $\alpha = 4$ (arbitrary value). Note that the critical value $\alpha = 41/30$ separates super-critical and subcritical bifurcations to Kerr combs.

a few events of high intensity indeed have a higher probability of occurrence than a standard Rayleigh or Gaussian distribution.

A convenient way to characterize rogue waves is to calculate the significant wave height (SWH), defined as the mean amplitude of the highest third of the waves. An event will qualify as a rogue wave provided its height is at least two times higher that the SWH [24]. In the $F^2 = 10$ and $F^2 = 20$, the SWH is equal to 20 and 25 respectively, and a few waves are of greater magnitude in both cases. Rogue waves have to fulfill this empirical criterion and the field map of Fig. 2 and Fig. 4 confirms that extreme events in the LLE are indeed precisely localized structures in the spatio-temporal representation. The interpretation of rogue waves as breathers collisions justifies the short durations that are observed in the simulations.

From a dynamical point of view, this phenomenology can be explained from the topology of the nonlinear resonance profile of the pumped mode. The angle-independent fixed points ψ_0 (or "flat states") of the system obey the algebraic equation $F^2 = [1 + (|\psi_0|^2 - \alpha)^2]\,|\psi_0|^2$, which is cubic in $|\psi_0|^2$. The corresponding resonance profiles for different excitations F^2 are displayed in Fig. 5 (b), and the solutions $|\psi_0|^2$ for $\alpha = 4$ are marked with dots. Rogue waves appear when the upper flat solution is the only one possible, or when the lower solution cannot sustain the presence of spatial structures like solitons or breathers. The figurative point of the system is therefore located above or in the vicinity of the 0^2 bifurcation line in the α–F^2 plane (see Fig. 5 (a)).

In conclusion, we have presented in this work theoretical evidence of optical rogue waves in WGM resonators pumped by a continuous-wave laser field. The spatiotemporal evolution of the intra-cavity field has been modelled using the Lugiato-Lefever equation. We have focused on the conditions leading to the generation of extreme events, and the detuning was chosen in a way such that solitons can emerge from the noisy initial condition. As the continuous pump power is increased, extreme events are numerically observed. These events are characterized by shorter duration, amplitudes larger than twice the SWH, and higher probabilities than that of a standard Rayleigh or Gaussian statistics These rogue waves therefore appear to emerge from the interaction between cavity soliton breathers, and since this physical system can be controlled with great accuracy, we expect this study to seed a comprehensive understanding of extreme events from a generic standpoint.

J. M. D. and Y. K. C. acknowledge financial support from the European Research Council through the projects ERC AdG MULTIWAVE and ERC StG NextPhase, respectively.

[1] N. Akhmediev and E. Pelinovsky (Eds.), "Rogue waves - Towards a unifying concept", special issue of the Eur. Phys. J. Spe. Top. (2010).
[2] D. R. Solli, C. Ropers, P. Koonath, and B. Jalali, Nature **450**, 1054 (2007).
[3] B. Kibler, J. Fatome, C. Finot, G. Millot, F. Dias, G. Genty, N. Akhmediev, and J. M. Dudley, Nature Physics **6**, 790 (2010).
[4] M. G. Kovalsky, A. A. Hnilo, and J. R. Tredicce, Opt. Lett. **36**, 4449 (2011).
[5] C. Bonatto, M. Feyereisen, S. Barland, M. Giudici, C. Masoller, J. R. Rios Leite, and J. R. Tredicce, Phys. Rev. Lett. **107**, 053901 (2011),
[6] A. N. Pisarchik, R. Jaimes-Reategui, R. Sevilla-Escoboza, G. Huerta-Cuellar, and M. Taki, Phys. Rev. Lett. **107**, 274101 (2011),
[7] F. T. Arecchi, U. Bortolozzo, A. Montina, and S. Residori, Phys. Rev. Lett. **106**, 153901 (2011).
[8] J. M. Soto-Crespo, P. Grelu, and N. Akhmediev, Phys. Rev. E **84**, 016604 (2011).
[9] A. Zaviyalov, O. Egorov, R. Iliew, and F. Lederer, Phys. Rev. A **85**, 013828 (2012).
[10] C. Lecaplain, P. Grelu, J. M. Soto-Crespo, and N. Akhmediev, Phys. Rev. Lett. **108**, 233901 (2012).

[11] N. Akhmediev, J. M. Dudley, D. R. Solli, and S. K. Turitsyn, J. Opt. **15**, 060201 (2013)
[12] A. B. Matsko, A. A. Savchenkov, W. Liang, V. S. Ilchenko, D. Seidel, and L. Maleki, Opt. Lett. **36**, 2845 (2011).
[13] Y. K. Chembo and C. R. Menyuk, Phys. Rev. A **87**, 053852 (2013).
[14] S. Coen, H. G. Randle, T. Sylvestre, and M. Erkintalo, Opt. Lett. **38**, 37 (2013).
[15] L. A. Lugiato and R. Lefever, Phys. Rev. Lett. **58**, 2209 (1987).
[16] A. Coillet, I. Balakireva, R. Henriet, K. Saleh, L. Larger, J. Dudley, C. Menyuk, and Y. K. Chembo, IEEE Photonics Journal **5**, 6100409 (2013).
[17] S. Coen and M. Erkintalo, Opt. Lett. **38**, 1790 (2013).
[18] Y. K. Chembo, D. V. Strekalov, and N. Yu, Phys. Rev. Lett. **104**, 103902 (2010.
[19] Y. K. Chembo and N. Yu, Phys. Rev. A **82**, 033801 (2010).
[20] T. Herr, V Brasch, J. D. Jost, C. Y. Wang, N. M. Kondratiev, M. L. Gorodetsky, T. J. Kippenberg, *arXiv:1211.0733v3*, June 2013.
[21] F. Leo, L. Gelens, P. Emplit, M. Haelterman, and S. Coen, Opt. Express **21**, 9180 (2013).
[22] C. Godey, I. Balakireva, A. Coillet, and Y. K. Chembo, arXiv:1308.2539 (2013).
[23] I. Balakireva, A. Coillet, C. Godey, and Y. K. Chembo, arXiv:1308.2542 (2013).
[24] M. Erkintalo, G. Genty and J.M. Dudley, Eur. Phys. J. Special Topics **185**, 135–144 (2010).